

# Zero sound density oscillations in Fermi-Bose mixtures

P. Capuzzi and E. S. Hernández\*

*Departamento de Física, Facultad de Ciencias Exactas y Naturales, Universidad de Buenos Aires, RA-1428 Buenos Aires, Argentina*

Within a mean field plus Random-Phase Approximation formalism, we investigate the collective excitations of a three component Fermi-Bose mixture of K atoms, magnetically trapped and subjected to repulsive  $s$ -wave interactions. We analyze both the single-particle excitation and the density oscillation spectra created by external multipolar fields, for varying fermion concentrations. The formalism and the numerical output are consistent with the Generalized Kohn Theorem for the whole multispecies system. The calculations give rise to fragmented density excitation spectra of the fermion sample and illustrate the role of the mutual interaction in the observed deviations of the bosonic spectra with respect to Stringari's rule.

03.75.Fi, 05.30.Fk, 32.80.Pj, 21.60.Jz

## I. INTRODUCTION

Shortly after the achievement of Bose-Einstein condensation of dilute, magnetically confined alkali atoms, an experimental quest began, seeking to trap and cool fermionic isotopes of lithium and potassium below their Fermi degeneracy temperatures  $T_F$  [1–4]. The first realization of a weakly interacting, degenerate Fermi gas of K atoms was reported by DeMarco and Jin [5], and most recently, a mixture of bosonic and fermionic Li isotopes has been sympathetically cooled to about 80% of the corresponding  $T_F$  [6]. On the theoretical side, various studies of the structure and equilibrium density profiles of harmonically confined fermions were anticipated in the last years [7], as well as thermodynamic properties [8]. The coexistence of trapped bosonic and fermionic isotopes of a given element received particular attention [9–15], mostly seeking to establish the effects of quantum degeneracy and mutual interaction on the respective density profiles, energetics and stability properties.

Since the early days of Bose-Einstein condensates, theoretical and experimental investigation of the excitation spectra of these objects constituted a field of active research (see, for example, Refs. [16,17] for substantial reviews) which largely enriched with reciprocal feedback. In spite of the lack of experimental data concerning trapped degenerate fermion gases, theoretical study of their collective oscillations also developed according to two viewpoints. On the one hand, a hydrodynamic approach derived from the balance equations for the moments of the Wigner distribution function permitted to compute the sound mode spectrum of one [18] and two [19] hyperfine fermion species. Such an approach, which can be generalized for anisotropically trapped systems [20] and was applied as well to predict the characteristics of scissor modes in a superfluid Fermi gas [21], conceals the hypothesis of underlying local equilibrium of the oscillating gas, i.e., the validity of the Fermi gas equation of state. On the other hand, since collision rates in a very cold and strongly dilute gas are small for moderate num-

bers of confined particles [19,22], one may expect that a zero sound regime shows up at low excitation energies and temperatures in these systems; in fact, collective energies of a single-species fermion gas were estimated within a sum-rule approach [23] for the lowest multiplicities. Recently, we have proposed a Hartree-Fock (HF) plus Random-Phase-Approximation (RPA) description of multipolar excitations of two hyperfine components of  $^{40}\text{K}$  atoms, mutually coupled through a repulsive  $s$ -wave interaction [24]. The procedure proved adequate to obtain the trend of collective energies and transition densities for multiplicities  $L = 0, 1, 2$ , both for the density and spin density oscillations, and the results were satisfactorily checked against a simple model, which permits analytical predictions in the case of identical trapping potentials and particle numbers for either component. Moreover, the philosophy turned out to be equivalent to the one undertaken by Bruun [25] for Li atoms interacting through an attractive coupling.

Due to their coexistence in natural samples, the possibility of simultaneous trapping and thermal equilibration of both bosonic and fermionic isotopes of a given alkali within their respective degeneracy regimes, makes room to an interesting field for theoretical anticipation, where the study of excitations of these binary mixtures constitute an open issue. This subject has not been pursued in depth, as compared with the interest deposited in structural characteristics and energetics. A three fluid model for trapped fermions coexisting with both condensed and noncondensed bosons was applied in Ref. [10] to the study of the temperature dependent profiles, and in Ref. [15] to outline a study of density fluctuations within the hydrodynamic regime. Some features of collisionless, zero sound oscillations in the Landau limit have been discussed in Ref. [14] and in Ref. [26], a sum-rule approach was applied to extract the lowest collective zero sound energies of an isotopic mixture of K atoms.

The purpose of the present work is to contribute to this wide field reporting calculations of the zero sound spectrum of trapped, weakly interacting K isotopes - ei-

ther bosonic  $^{39}\text{K}$  or  $^{41}\text{K}$ , together with two hyperfine species of  $^{40}\text{K}$ . The theoretical frame is the mean field-plus-RPA for the coupled threefold system at zero temperature, which is exposed in Sec. II within a simplified scope. The results here presented then indicate the trend to be expected at very low temperatures, when quantum degeneracy overcomes the effects of interactions in the fermion sample, and should be revised if the fermionic gas lies in its superfluid regime. The procedure can be extended to finite temperatures, at some computational cost. Specific calculations are analyzed in Sec. III, while the conclusions and overview of this paper are the subject of Sec. IV.

## II. THE PHYSICAL SYSTEM

As anticipated in the Introduction, in this work we study a cold dilute K gas with three components, confined in a spherical harmonic potential. Two of the components, hereafter called species 1 and 2, are fermions with different spin projections and the third one is a boson  $B$  species. Although in principle, different components subjected to the same magnetic field would effectively feel different trapping potentials, we have assumed, for simplicity, that all atoms experience the same confinement

$$V_{\text{trap}} = \frac{1}{2}m\omega^2 r^2 \quad (2.1)$$

where  $m$  is the atom mass, in other words, we neglect minor mass differences among potassium isotopes, as well as variations in the trap frequency due to the distinct spin projections. In addition to the external field, the atoms can interact, but due to the diluteness and temperature of the gas sample it is enough to consider only  $s$ -wave interactions [17]. Since our gas includes two types of identical fermions, *not* all  $s$ -scattering processes are permitted; in fact, each fermion species is a free Fermi gas which can only interact with atoms of a different kind.

Taking into account that the  $s$ -wave interaction can be represented as a contact potential  $V_s = g\delta(\mathbf{r} - \mathbf{r}')$  with  $g = 4\pi a_s \hbar^2/m$ , being  $a_s$  the scattering length of the process, the mean-field Hamiltonians for the three species can be written as

$$\begin{aligned} H_B &= \frac{p^2}{2m} + \frac{1}{2}m\omega^2 r^2 + g_B \rho_B + g_1 \rho_1 + g_2 \rho_2, \\ H_1 &= \frac{p^2}{2m} + \frac{1}{2}m\omega^2 r^2 + g_f \rho_2 + g_1 \rho_B, \\ H_2 &= \frac{p^2}{2m} + \frac{1}{2}m\omega^2 r^2 + g_f \rho_1 + g_2 \rho_B, \end{aligned} \quad (2.2)$$

being  $g_B, g_1, g_2$ , and  $g_f$  the interaction strength between bosons, species 1 and B, species 2 and B, and species 1 and 2 respectively.

These Hamiltonians provide the single particle wavefunctions and energies necessary to find the equilibrium densities  $\rho_B, \rho_1, \rho_2$ , with  $\rho_B = N_B |\phi_0|^2$  and

$$\rho_\sigma = \sum_{nl} (2l+1) |\psi_{nl}^\sigma|^2 N(\varepsilon_{nl}^\sigma - \varepsilon_{F\sigma}), \quad (2.3)$$

for  $\sigma = 1, 2$ , being  $N(\varepsilon)$  the Fermi occupation numbers at given temperature  $T$ , and  $\varepsilon_{F\sigma}$  the Fermi energy of species  $\sigma$ , satisfying

$$N_{F\sigma} = \sum_{nl} (2l+1) N(\varepsilon_{nl}^\sigma - \varepsilon_{F\sigma}). \quad (2.4)$$

The particle eigenspectrum is the solution of the coupled equations

$$H_B \phi_{nlm} = \epsilon_{nl} \phi_{nlm}, \quad (2.5a)$$

$$H_\sigma \psi_{nlm}^\sigma = \varepsilon_{nl}^\sigma \psi_{nlm}^\sigma. \quad (2.5b)$$

It is worth mentioning that Eq. (2.5a) for  $n=0, l=0$  is the Gross-Pitaevskii equation (GPE) for  $N_B$  atoms with chemical potential  $\mu = \epsilon_0$  in an external potential  $V = V_{\text{trap}} + (g_1 \rho_1 + g_2 \rho_2)$ . The higher modes are the excitation modes of the GPE which must not be confused with the Hartree-Fock-Bogoliubov (HFB) modes.

### A. Collisionless approximation

To obtain the spectrum of collective excitations of the compound system we resort to a random phase approximation, which treats the three species on the same footing. In a previous work [24], we have derived two equivalent sets of two equations each, for the density fluctuations  $\delta\rho^{\sigma\sigma'}$ , being  $\sigma, \sigma'$  either 1 or 2. These represent the response of the density  $\rho_\sigma$  to an initial perturbation of  $\rho_{\sigma'}$ . The diagonal and off-diagonal density fluctuations can be later mapped onto spin symmetric and spin antisymmetric ones for each species and for the whole gas. A similar approach in the presence of the bosonic component would lead to nine equations which include transition densities  $\delta\rho^{BB}, \delta\rho^{\sigma B}, \delta\rho^{B\sigma}$  and corresponding ones for the other fermion species. In this work, we shall consider identical fermion numbers  $N_{F\sigma}$  in each species, and we are mostly interested in total transitions densities, namely

$$\begin{aligned} \delta\rho_\sigma &= \delta\rho^{\sigma\sigma} + \delta\rho^{\sigma\sigma'} + \delta\rho^{\sigma B}, \\ \delta\rho_B &= \delta\rho^{BB} + \delta\rho^{B\sigma} + \delta\rho^{B\sigma'}. \end{aligned} \quad (2.6)$$

Accordingly, from the full system of equations we can derive a simplified set, which turns out to be similar to the one developed by Minguzzi and Tosi for Bose-Einstein condensates at finite temperatures [27]. The details are outlined in Appendix A. In this frame, a density fluctuation evolves in a perturbed HF potential according to the linearized Hamiltonians in (2.2). In terms of the particle-hole (ph) propagators for each spin species in the HF approximation,  $G_0^\sigma$ , we get for the transition densities

$$\begin{aligned}
\delta\rho_\sigma(\mathbf{r}) &= \delta\rho_\sigma^0(\mathbf{r}) \\
&+ \int G_0^\sigma(\mathbf{r}, \mathbf{r}') [g_\sigma \delta\rho_B(\mathbf{r}') + g_f \delta\rho_{\sigma'}(\mathbf{r}')] d^3r', \\
\delta\rho_B(\mathbf{r}) &= \delta\rho_B^0(\mathbf{r}) \\
&+ \int G_0^B(\mathbf{r}, \mathbf{r}') \left[ g_B \delta\rho_B(\mathbf{r}') + \sum_\sigma g_\sigma \delta\rho_\sigma(\mathbf{r}') \right],
\end{aligned} \tag{2.7}$$

where  $\delta\rho_i^0$  is the density fluctuation induced by the external probe  $O^\dagger$  in the stationary HF mean-field approximation

$$\delta\rho_i^0(\mathbf{r}) = \int O^\dagger(\mathbf{r}') G_0^i(\mathbf{r}, \mathbf{r}') d^3r', \tag{2.8}$$

and the propagators read

$$\begin{aligned}
G_0^B &= N_B \sum_{j \neq 0} \left\{ \frac{\phi_0(\mathbf{r}') \phi_0^*(\mathbf{r}) \phi_j(\mathbf{r}) \phi_j^*(\mathbf{r}')}{\Omega - (\epsilon_j - \mu)/\hbar + i\eta} \right. \\
&\quad \left. - \frac{\phi_0(\mathbf{r}) \phi_0^*(\mathbf{r}') \phi_j(\mathbf{r}') \phi_j^*(\mathbf{r})}{\Omega + (\epsilon_j - \mu)/\hbar + i\eta} \right\},
\end{aligned} \tag{2.9a}$$

$$\begin{aligned}
G_0^\sigma &= \sum_{j k} \frac{N(\epsilon_k^\sigma - \epsilon_{F\sigma}) - N(\epsilon_j^\sigma - \epsilon_{F\sigma})}{\Omega - (\epsilon_j^\sigma - \epsilon_k^\sigma)/\hbar + i\eta} \\
&\quad \psi_j^{\sigma*}(\mathbf{r}') \psi_j^\sigma(\mathbf{r}) \psi_k^{\sigma*}(\mathbf{r}) \psi_k^\sigma(\mathbf{r}'),
\end{aligned} \tag{2.9b}$$

where each single particle label stands for  $n, l, m$ , and the condensate mode is excluded from the summation in (2.9a).

It is clear that in the present situation, i.e.,  $N_{F1} = N_{F2}$  and identical trapping field for both hyperfine components, one has a single fermion spectrum  $\epsilon_{nl}^\sigma \equiv \epsilon_{nl}^F$ , one ph propagator  $G_0^\sigma \equiv G_0^F$  and same fluctuations  $\delta\rho_\sigma \equiv \delta\rho_F$ . Due to the spherical symmetry imposed to the trapping potential and for multipolar operators  $O^\dagger$ , Eqs. (2.7) can be rewritten in terms of multipolar components as

$$\begin{aligned}
\delta\rho_\sigma^l(r) &= \delta\rho_\sigma^{0l}(r) + \frac{4\pi}{2l+1} \int r'^2 dr' G_{0l}^F(r, r') \\
&\quad [g_\sigma \delta\rho_B^l(r') + g_f \delta\rho_{\sigma'}^l(r')], \\
\delta\rho_B^l(r) &= \delta\rho_B^{0l}(r) + \frac{4\pi}{2l+1} \int r'^2 dr' G_{0l}^B(r, r') \\
&\quad [g_B \delta\rho_B^l(r') + \sum_\sigma g_\sigma \delta\rho_\sigma^l(r')],
\end{aligned} \tag{2.10}$$

where the expressions for the  $l$ -polar propagators  $G_{0l}^i$  are given in Appendix B and the total density fluctuation for type  $i$ -atoms reads

$$\delta\rho_i(\mathbf{r}) = \sum_l Y_{l0}(\hat{r}) \delta\rho_i^l(r), \tag{2.11}$$

being  $Y_{lm}$  standard spherical harmonic functions.

The whole process consists of three stages. First, one has to find the equilibrium densities, which means to solve the GPE coupled to the fermionic system of HF equations. This calculation also yields the quasi-particle spectrum of the fermions. Then, one computes the GPE excitations for the bosons, and finally, one solves the RPA equations (2.10) for the density fluctuations with given  $l$ . After computing the transition densities, we calculate the total susceptibility ( $\chi$ ) and dynamic structure factor ( $S$ ) of the system as

$$\begin{aligned}
\chi^l(\Omega) &= \chi_B^l + \chi_1^l + \chi_2^l, \\
S^l(\Omega) &= -\frac{1}{\pi} \text{Im} [\chi^l],
\end{aligned} \tag{2.12}$$

with  $\chi_i^l$  the susceptibility of each component in the interacting system,

$$\chi_i^l = \begin{cases} \int r^{2+l} \delta\rho_i^l(r) dr & l \neq 0 \\ \int r^4 \delta\rho_i^0(r) dr & l = 0 \end{cases} \tag{2.13}$$

From the poles of the real part of  $\chi^l$  or corresponding peaks in  $S$  we can extract the excitation energies of the collective modes.

### III. RESULTS

In this work, we analyze the spectrum of elementary and collective excitations for varying concentrations of the fermionic species. For this sake, we tune the parameters close to the experimental setup of DeMarco *et al.* [5], i.e., we choose  $\omega = 2\pi \times 70 \text{ s}^{-1}$ ,  $a_1 = a_2 = 2.519 \text{ nm}$ ,  $a_f = 8.308 \text{ nm}$  and  $a_B = 4.292 \text{ nm}$ , corresponding to  $^{40}\text{K}$  (fermions) atoms and  $^{39}\text{K}$  (bosons).

The computation of the single-particle (sp) spectrum, Eq. (2.5), was carried out by expanding their eigen-solutions in a basis of harmonic oscillator functions with 1800 radial wavefunctions. In fact, due to the spherical symmetry of the trap, we have just diagonalized several small systems for different  $l$  ( $l \lesssim 60$ ). Convergence was achieved with an accuracy of at least  $10^{-10}$  in the energies, and the coincidence between  $\mu$  and  $\epsilon_0$  was checked to about  $10^{-5}$ . Then, the numerical solution of Eq. (2.10) for each  $\Omega$  and  $L$  was performed by discretizing the problem in a spatial mesh containing up to 250 points and extending up to  $R \approx 30 \mu\text{m}$  (approximately fifteen oscillator sizes); the resulting linear system was solved with standard routines from the LAPACK Fortran library.

In the next subsections we analyze both the quasi-particle spectrum and the selfconsistent RPA collective modes. We use the notation  $N_F$  for either  $N_{F\sigma}$  and  $g_\sigma$  for the common coupling  $g_1 = g_2$ .

## A. Hartree-Fock and GPE excitations

Within the mean field approach to the coupled system we calculated the quasi-particle excitations according to Eqs. (2.5). The main features of the HF fermionic energies are the following: for low numbers of fermions in the trap,  $N_F \lesssim 10^4$ , the excitations energies of the pure fermion system are basically the harmonic oscillator ones. When we turn on the coupling to the bosonic component, the repulsion with the condensate increases the Fermi energy and lowers the slope of the dispersion relation. The change in slope is more significant, the larger the difference  $N_B - N_F$ ; indeed, it becomes unimportant when these numbers are comparable or slightly negative.

As shown by Mølmer [9], for high number of bosons, their kinetic and interaction energies with the fermions can be neglected in  $H_B$ , yielding a Thomas-Fermi approximated (TFA) [28] bosonic particle density

$$\rho_B = N_B |\phi_0|^2 = \frac{1}{g_B} (\mu - V_{\text{trap}}) \Theta(\mu - V_{\text{trap}}), \quad (3.1)$$

where  $\Theta(x)$  is the step function. This is translated, after replacement in the fermionic Hamiltonian [cf. Eqs. (2.2)], into a wider harmonic trap, shifted upwards according to

$$V_{\text{eff}} = V_{\text{trap}} + \frac{g_\sigma}{g_B} (\mu - V_{\text{trap}}) \Theta(\mu - V_{\text{trap}}), \\ = \begin{cases} \frac{g_\sigma}{g_B} \mu + V_{\text{trap}} (1 - \frac{g_\sigma}{g_B}) & \text{if } r < R_B \\ V_{\text{trap}} & \text{otherwise} \end{cases} \quad (3.2)$$

with the Bose radius in the TFA,  $R_B = \sqrt{2\mu/m\omega^2}$ . For the values of the coupling constants here considered, the strength of the restoring force experienced by fermions inside the bosonic cloud is reduced by a factor  $(1 - g_\sigma/g_B) \approx 0.41$ . Consequently, the Fermi radius  $R_F = \sqrt{2\varepsilon_F/m\omega^2}$  acquires an effective value

$$R_{F \text{ eff}} = \sqrt{\frac{2(\varepsilon_F - \mu g_\sigma/g_B)}{(1 - g_\sigma/g_B)m\omega^2}}, \quad (3.3)$$

which increases with respect to its size in a pure fermion system. The low-lying quasi-particle excitations—i.e. those with energies below the chemical potential  $\mu$  of the bosons—are then expected to be sensitive to the renormalized trapping strength, whereas the higher energy ones, which extend further beyond the central region, are less affected by the effective trapping. In Fig. 1 we plot the dispersion relation for  $N_F = 9880$ , and several values of  $N_B$ . The corresponding values of the boson chemical potential are indicated in the caption. We observe that, in agreement with the effective trapping picture, when the bosonic cloud is large enough, the low lying modes increase with a smaller slope than the modes with energies higher than  $\mu$ . Although the fermionic spectrum is altered by the interaction, the bosonic counterpart is almost unchanged; indeed, in addition to the different number of particles in each isotope, the fermionic

character of the  $^{40}\text{K}$  atoms gives rise to quasi-particle excitations rather sensitive to variations in the effective trap. The bosonic spectrum is very different; it actually consists of the GPE single-particle excitations which will build the collective energies in a RPA calculation.

## B. Random-Phase Approximation

The general aspect of the response (2.12) can be interpreted from its constituents. Without the boson-fermion coupling, i.e.  $g_1 = g_2 = 0$ , the bosonic response consists of the well-known collective excitations enclosed in the zero temperature Gross-Pitaevskii equation (2.5a), namely, the HFB spectrum mentioned immediately above Sec. II A. For high number of bosons, this is well reproduced by Stringari's hydrodynamic formulation [28], which provides an analytic expression for the multipolar excitation energies. Although analytic formulae have been also found for systems of interacting fermions [15,21], they hold in the hydrodynamic regime and for population ranges far from those we address here, so we compare our results with earlier numerical calculations carried within the collisionless regime.

We have analyzed the dynamic structure factors and fluctuations created by multipolar external fields with  $L = 0, 1, 2$ . In Fig. 2 we show the monopolar spectrum for several values of  $N_B$  and  $N_F$ . The essential features of the monopolar response can be summarized as follows.

1. Fixed  $N_F$ : for high  $N_B$  (higher rows), the spectrum is dominated in amplitude by the bosonic collective modes with frequencies  $\Omega \approx \sqrt{5}, \sqrt{14}, \dots$  [cf. Ref. [28]]. However, strong fragmentation occurs near the fermionic RPA poles, which can be visualized in the lowest row. As we lower  $N_B$ , this fragmentation is reduced and two sets of two peaks each is distinguished, each set corresponding to the bosonic and fermionic constituents. The bosonic peak separates from the Stringari spectrum towards the ideal gas result  $\Omega = 2n\omega$ , revealing the unimportant role of both the boson-boson and boson-fermion interaction in this very dilute regime. The fragmentation in the fermionic part cannot be seen due to its weakness and the current energy scale.
2. Fixed  $N_B$ : one realizes that increasing  $N_F$  not always yields a more fragmented spectrum. In fact, some peaks appear better defined for larger values of  $N_F$ , while other states seem to spread over a larger energy range. On the other hand, one should keep in mind that the scale in this plot is governed by the boson strength. If this scale is released, one may observe the pure fermion RPA peaks (i.e., those with  $N_B = 0$ ) within restricted intervals, with fragmented structures for sufficiently high  $N_F$ .

The results for the dipolar mode ( $L = 1$ ) displayed in Fig. 3 are somewhat different. As we can see, for all

values of  $N_B$  and  $N_F$  the highest peak lies at  $\Omega = \omega$ , corresponding to a center-of-mass (Kohn mode) oscillation of the *whole* system. It is known [24,29,30] that both the pure boson and pure fermion systems possess a well defined Kohn mode within the RPA formulation, which is recovered in the fully coupled calculation, as can be seen in Fig. 3. In fact, in the numerical calculations the precise location of this pole has been used to check the computational code. It should be mentioned, however, that in a actual experimental setup, the slight differences between the trap forces for each constituents would distort these modes, giving rise to coupled oscillation of the components. In addition, the dipolar spectrum is highly fragmented around  $\Omega = 3\omega$ , which coincides with an oscillator mode for  $l = 1$ . As in the monopole case, the important fragmentation seems to disappear as we lower either  $N_B$  or  $N_F$ .

The quadrupolar mode exhibits the strongest fragmentation. Even for low values of  $N_B$  and  $N_F$  the spectrum presents several major peaks whose number grows at higher densities. At the highest population of all species, the largest peak corresponds to a boson excitation with  $\Omega \approx \sqrt{2}\omega$  in agreement with the sum-rule estimate of Ref. [26]. As we diminish the number of bosons the peak is shifted upwards towards the ideal gas value  $\Omega = 2\omega$ . Another feature not seen in other multipolarities is the existence of peaks with substantial strength at rather low energies near  $\Omega \approx 0.3\omega$ .

The shape of the transition densities deserves its own study. In Fig. 5 we depict the monopolar fluctuations corresponding to the frequencies where the maximum transition probability is attained, each curve has been independently scaled to fit in the plot. Apart from differences in scale, the shapes of the bosonic fluctuations are very similar for all  $N_B$  and  $N_F$ , displaying in any case a volume-like excitation with nonvanishing density at the origin. However, two kinds of fermionic excitations can be seen, a volume-like one, similar to the bosonic mode, and another which oscillates between the boundaries  $R_{F\text{eff}}$  and  $R_B$  of the isotopic particle densities. These two shapes can be correlated to the spectrum [see Fig. 2]: while the volume-like fluctuations occur for essentially pure boson peaks and in configurations where the bosonic cloud surrounds the fermionic component, the surface-like mode appears near the pure fermion excitation. The fermionic atoms extend outwards with respect to the bosonic density and the excitation bounces between the fermionic and bosonic density boundaries. To support this idea we have tabulated the radius of both densities in Table I.

The monopolar response contains other types of density fluctuations, some of them correspond to important poles in the response; one can observe not only volume-like bosonic excitations, but also surface-like ones, in spatial counterphase to the fermionic ones for the frequencies shown.

As expected from the Generalized Kohn Theorem, the dipolar fluctuations at trap frequency do exist and correspond to a small displacement of the density yielding

a density fluctuation proportional to the gradient of the density, i.e.

$$\delta\rho_i^{l=1}(r, \Omega = \omega) \propto \frac{\partial\rho_i}{\partial r}. \quad (3.4)$$

For high enough  $N_B$ , according to the TFA, the bosonic density shape inside the condensate is parabolic, giving a linear  $\delta\rho$ . This is seen in Fig. 6 where we plot the fluctuation densities corresponding to these modes for  $N_B = 10^6$  and  $N_F = 969$ . The shape of the fermionic fluctuation is not as simple, and in fact, should not have a linear dependency with position since the TFA density profile carries a power 2/3. Moreover, the oscillatory shape shown in the plot agrees very well with the derivative of the fermionic density calculated within the HF approximation.

Finally, the behavior of the  $L = 2$  density fluctuations is similar to the monopolar ones in the sense that for large number of bosons and few fermions, the highest peak in the response corresponds to a fluctuation which extends over the bulk of the cloud; whereas for low boson number and/or many fermions, the fermionic fluctuation is mainly surface-like. The difference with  $L = 0$  lies in the fact that the quadrupolar oscillation vanishes smoothly at origin.

#### IV. CONCLUSIONS AND OVERVIEW

In this work we have designed a mean field plus RPA formalism for a trapped Fermi-Bose mixture, i.e., a three component gas at vanishing temperature. We have analyzed both the single-particle excitation spectra and the collisionless collective modes. On the one hand, the fermionic single-particle spectra can be interpreted in terms of an effective confining field induced by the presence of the bosonic atoms plus the trapping potential [9–11]. This effective field produces a packing of sp in the lowest branch of the spectrum. On the other hand, the bosonic part of the spectrum is mainly unaffected by a moderate fermionic cloud.

The poles of the monopolar and quadrupolar response are shifted away from either the pure fermion or pure boson results and the whole spectrum is highly fragmented, specially for the quadrupolar probe. In addition, for the dipolar excitation, the formalism proves to be theoretically and numerically consistent with the Generalized Kohn Theorem and the density fluctuations are proportional to the derivative of the corresponding equilibrium densities. The shape of the monopolar fluctuations reflects two kind of behaviors. For high number of bosons, both the fermionic and bosonic fluctuations are volume-like, extending up to their respective densities edges, while for similar number of particles, although the bosonic fluctuation remains volume-like, the fermionic counterpart bounces between both density borders.

Finally, this formalism can be extended to finite temperatures where the system may be found partially degenerate, i.e. with the bosonic and/or fermionic components out of the quantum degeneracy regime. This new regime could give rise to an interesting and rich field of research.

## ACKNOWLEDGMENTS

This paper was supported by Grant No. TW81 from the Universidad of Buenos Aires (UBA). One of us (P.C.) is grateful to the Universidad de Buenos Aires for financial support.

## APPENDIX A: RANDOM PHASE APPROXIMATION

We assume that the trapped, three component atom system is excited by the action of an external field, so that ph pairs ( $\alpha\beta$ ) involving, in principle, both hyperfine fermion species and the bosons, are created. We also suppose that a ph effective interaction  $V_{\text{ph}}^{\alpha\beta\gamma\delta}$ , that permits propagation of elementary excitations carrying energy  $\Omega$  to all orders in the interaction, gives rise to the dressed RPA propagator for ph pairs [31]

$$G^{\alpha\beta}(\Omega) = G_0^{\alpha\beta}(\Omega) + \sum_{\gamma\delta} G_0^{\alpha\beta}(\Omega) V_{\text{ph}}^{\alpha\beta\gamma\delta} G^{\gamma\delta}(\Omega). \quad (\text{A1})$$

We consider longitudinal excitations involving propagation of ph pairs of the same spin kind, created by multipolar operators of the form

$$O^\dagger = \begin{cases} r^L Y_{L0}(\theta, \varphi) & L \neq 0 \\ r^4 Y_{00} & L = 0, \end{cases} \quad (\text{A2})$$

and an effective interaction which couples ph pairs of i) different fermion species, expressed as  $V_{\text{ph}}^{\sigma\sigma'} \equiv V_{\text{ph}}^{\sigma\sigma\sigma'\sigma'}$ ; ii) each fermion species and the bosons,  $V_{\text{ph}}^{\sigma B} \equiv V_{\text{ph}}^{\sigma\sigma BB}$  and iii) bosons,  $V_{\text{ph}}^{BB}$ . The free ph propagators involved in longitudinal density fluctuations are then diagonal in spin space and Eq. (A1) gives rise to nine coupled equations. After convoluting the propagators with the external field, one gets an equivalent system for the density fluctuations, which in matrix form can be cast as namely

$$\begin{aligned} \delta\rho^{\sigma\sigma} &= \delta\rho_0^{\sigma\sigma} + G_0^{\sigma\sigma} (g_f \delta\rho^{\sigma'\sigma} + g_\sigma \delta\rho^{B\sigma}), \\ \delta\rho^{\sigma'\sigma} &= G_0^{\sigma'\sigma} (g_f \delta\rho^{\sigma\sigma} + g_\sigma \delta\rho^{B\sigma}), \\ \delta\rho^{B\sigma} &= G_0^{BB} (g_\sigma \delta\rho^{\sigma\sigma} + g_{\sigma'} \delta\rho^{\sigma'\sigma} + g_B \delta\rho^{B\sigma}), \\ \delta\rho^{\sigma B} &= G_0^{\sigma\sigma} (g_f \delta\rho^{\sigma'B} + g_\sigma \delta\rho^{BB}), \end{aligned} \quad (\text{A3})$$

plus four similar equations corresponding to interchanging  $\sigma$  and  $\sigma'$ , in addition to the modified boson RPA equation

$$\begin{aligned} \delta\rho^{BB} &= \delta\rho_0^{BB} + G_0^{BB} (g_B \delta\rho^{BB} + g_\sigma \delta\rho^{\sigma B} \\ &+ g_{\sigma'} \delta\rho^{\sigma'B}). \end{aligned} \quad (\text{A4})$$

Under the conditions specified in this work, in other words, identical trapping potentials and same number of fermion of each hyperfine type, the fermion propagators are identical and one can easily construct the equations for the total density fluctuations of the fermionic and bosonic atoms, summing over the hole partner

$$\delta\rho_\alpha = \sum_\beta \delta\rho^{\alpha\beta}. \quad (\text{A5})$$

The final expressions are displayed in Eqs. (2.7).

## APPENDIX B: MULTIPOLAR DECOMPOSITION

To evaluate the free ph propagator we use the 3D basis functions calculated according to Eq. (2.5). These eigenfunctions can be written, for each species, as

$$\begin{aligned} \phi_{nlm}(\mathbf{r}) &\equiv R_{nl}(r) Y_{lm}(\hat{r}), \\ \psi_{nlm}^\sigma(\mathbf{r}) &\equiv R_{nl}^\sigma(r) Y_{lm}(\hat{r}), \end{aligned} \quad (\text{B1})$$

where  $Y_{lm}$  are spherical harmonic functions and  $R_{nl}^i$  the corresponding radial eigenfunctions.

Decomposing the propagators Eqs. (2.9) as

$$G_0^i(\mathbf{r}, \mathbf{r}', \Omega) = \sum_L G_{0L}^i P_L(\hat{r} \cdot \hat{r}'), \quad (\text{B2})$$

with  $P_L(u)$  Legendre polynomials of order  $L$ . The multipolar component  $G_{0L}^i$  read

$$\begin{aligned} G_{0L}^\sigma &= \frac{1}{(4\pi)^2} \sum_{\substack{n'l \\ n'l'}} R_{nl}^\sigma(r) R_{n'l'}^\sigma(r) R_{nl}^\sigma(r') R_{n'l'}^\sigma(r') \\ &(2l+1)(2l'+1) | \langle l0l'0 | l0 \rangle |^2 \chi_{nl,n'l'}^\sigma(\Omega), \end{aligned} \quad (\text{B3})$$

being

$$\chi_{nl,n'l'}^\sigma(\Omega) = \frac{N(\varepsilon_{nl} - \varepsilon_{F\sigma}) - N(\varepsilon_{n'l'} - \varepsilon_{F\sigma})}{\Omega - (\varepsilon_{nl} - \varepsilon_{n'l'})/\hbar + i\eta}, \quad (\text{B4})$$

and

$$\begin{aligned} G_{0L}^B &= N_B \phi_0(r) \phi_0(r') \frac{1}{4\pi} \sum_n' R_{nL}(r) R_{nL}(r') \\ &\left\{ \frac{1}{\omega - (\varepsilon_{nL} - \mu)/\hbar + i\eta} - \frac{1}{\omega + (\varepsilon_{nL} - \mu)/\hbar + i\eta} \right\}, \end{aligned} \quad (\text{B5})$$

where the primed summation in Eq. (B5) indicate to exclude the condensate mode, i.e  $n \geq 1$  for  $L = 0$ . Similarly, the  $l$ -polar density fluctuation read

$$\delta\rho_i^{0L}(r) = \frac{4\pi}{2L+1} \begin{cases} \int r'^{2+L} G_{0L}^i(r') dr' & L \neq 0 \\ \int r'^4 G_{00}^i(r') dr' & L = 0. \end{cases} \quad (\text{B6})$$

## APPENDIX C: SIMPLE PROOF OF THE KOHN MODE

The Kohn theorem states that, independently of the interactions, a many-body system subjected to a harmonic confinement possesses an excited state corresponding to an oscillation of its center-of-mass at the bare oscillator frequency  $\Omega = \omega$ . Consequently, the fulfillment of Kohn's theorem is a desired feature of any approximate formulation.

The RPA equations (A3) and (A4) can be cast in a  $9 \times 9$  matrix form, namely

$$\bar{\varepsilon} \cdot \delta\bar{\rho} = \delta\bar{\rho}_0, \quad (\text{C1})$$

with  $\delta\bar{\rho} = (\delta\rho^{11}, \delta\rho^{21}, \delta\rho^{B1}, \delta\rho^{12}, \delta\rho^{22}, \delta\rho^{B2}, \dots)^t$ , and

$$\bar{\varepsilon} = \begin{pmatrix} \mathbb{A} & 0 & 0 \\ 0 & \mathbb{A} & 0 \\ 0 & 0 & \mathbb{A} \end{pmatrix}, \quad (\text{C2})$$

being

$$\mathbb{A} = \begin{pmatrix} 1 & -g_f G_0^1 & -g_1 G_0^1 \\ -g_f G_0^2 & 1 & -g_2 G_0^2 \\ -g_1 G_0^B & -g_2 G_0^B & 1 - g_B G_0^B \end{pmatrix}. \quad (\text{C3})$$

The collective states of the system are located at the frequencies  $\Omega$  which give a singular matrix  $\bar{\varepsilon}$ , implying a singular  $\mathbb{A}$ . In addition, finding an eigenmode of  $\mathbb{A}$  with zero eigenvalue we prove that  $\mathbb{A}$  is singular. Moreover, solving this eigensystem is equivalent to solve Eq. (2.7) with  $\delta\rho_i^0$  set to zero.

We propose the solution

$$\delta\bar{\rho}(\omega) = \left( \frac{\partial\rho_1}{\partial x_j}, \frac{\partial\rho_2}{\partial x_j}, \frac{\partial\rho_B}{\partial x_j} \right)^t, \quad (\text{C4})$$

(for any direction  $j$ ) and using the fact that  $G_0^i$  is built of single-particle excitations corresponding to the mean-field Hamiltonians (2.2) we find [32]

$$\begin{aligned} \int G_0^\sigma(\mathbf{r}, \mathbf{r}', \omega) \left[ g_\sigma \frac{\partial\rho_B}{\partial x'_j} + g_f \frac{\partial\rho_{\sigma'}}{\partial x'_j} \right] d^3r' &= \frac{\partial\rho_\sigma}{\partial x_j}, \\ \int G_0^B(\mathbf{r}, \mathbf{r}', \omega) \left[ g_B \frac{\partial\rho_B}{\partial x'_j} + \sum_\sigma g_\sigma \frac{\partial\rho_\sigma}{\partial x'_j} \right] d^3r' &= \frac{\partial\rho_B}{\partial x_j}, \end{aligned} \quad (\text{C5})$$

which correspond to the requested eigensolution of  $\mathbb{A} \cdot \delta\bar{\rho} = \mathbf{0}$ .

---

\* Also at the Consejo Nacional de Investigaciones Científicas y Técnicas, Argentina.

- [1] F. S. Cataliotti, E. A. Cornell, C. Fort, M. Inguscio, F. Marin, M. Predevelli, L. Ricci, and G. M. Tino, *Phys. Rev. A* **57**, 1136 (1998).
- [2] M. Predevelli, F. S. Cataliotti, E. A. Cornell, J. R. Ensher, C. Fort, L. Ricci, G. M. Tino, and M. Inguscio, *Phys. Rev. A* **59**, 886 (1999).
- [3] W. I. McAlexander, E. R. I. Abraham, N. W. M. Ritchie, C. I. Williams, H. T. C. Stoof, and R. G. Hulet, *Phys. Rev. A* **51**, R871 (1995).
- [4] M.-O. Mewes, G. Ferrari, F. Schreck, A. Sinatra, and Ch. Salomon, *Phys. Rev. A* **61**, R011403 (2000).
- [5] B. DeMarco and D. S. Jin, *Science* **285**, 1703 (1999); B. DeMarco, S. B. Papp, and D. S. Jin, *cond-mat/0101445*, (2001).
- [6] F. Schreck, G. Ferrari, K. L. Corwin, J. Cubizolles, L. Khaykovich, M.-O. Mewes, and C. Salomon, *cond-mat/0011291*, (2000).
- [7] D. A. Butts and A. S. Rokhsar, *Phys. Rev. A* **55**, 4346 (1997); J. Schneider and H. Wallis, *Phys. Rev. A* **57**, 1253 (1998); G. M. Bruun and K. Burnett, *Phys. Rev. A* **58**, 2427 (1998).
- [8] J. M. B. Noronha and D. J. Toms, *Phys. Lett. A* **267**, 276-280 (2000).
- [9] K. Mølmer, *Phys. Rev. Lett.* **80**, 1804 (1998).
- [10] M. Amoruso, A. Minguzzi, S. Stringari, M. P. Tosi, and L. Vichi, *Eur. Phys. J. D* **4**, 261 (1998).
- [11] L. Vichi, M. Inguscio, S. Stringari, and G. M. Tino, *J. Phys. B: At. Mol. Opt. Phys.* **31**, L899-L907 (1998).
- [12] L. Vichi, M. Amoruso, A. Minguzzi, S. Stringari, and M. P. Tosi, *Eur. Phys. J. D* **11**, 335-339 (2000).
- [13] N. Nygaard and K. Mølmer, *Phys. Rev. A* **59**, 2974 (1999).
- [14] L. Viverit, C. J. Pethick, and H. Smith, *Phys. Rev. A* **61**, 053605 (2000).
- [15] A. Minguzzi and M. P. Tosi, *Phys. Lett. A* **268**, 142-148 (2000).
- [16] F. Dalfovo, S. Giorgini, L. P. Pitaevskii, and S. Stringari, *Rev. Mod. Phys.* **71**, 463 (1999).
- [17] *Bose-Einstein condensation of atomic gases*, edited by M. Inguscio, S. Stringari, and C. E. Wieman, IOS press, Amsterdam, 1999.
- [18] M. Amoruso, J. Meccoli, A. Minguzzi, and M. P. Tosi, *Eur. Phys. J. D* **7**, 441 (1999).
- [19] M. Amoruso, J. Meccoli, A. Minguzzi, and M. P. Tosi, *Eur. Phys. J. D* **8**, 361 (2000).
- [20] A. Csordás and R. Graham, *Phys. Rev. A* **63**, 013606 (2000).
- [21] A. Minguzzi and M. P. Tosi, *Phys. Rev. A* **63**, 023609 (2001).
- [22] G. M. Bruun and C. W. Clark, *Phys. Rev. Lett.* **83**, 5415 (1999).
- [23] L. Vichi and S. Stringari, *Phys. Rev. A* **60**, 4734 (1999).
- [24] P. Capuzzi and E. S. Hernández, to appear *Phys. Rev. A* (2001).
- [25] G. M. Bruun, *Phys. Rev. A*, in press.
- [26] T. Miyakawa, T. Suzuki, and H. Yabu, *Phys. Rev. A* **62**, 063613 (2000).
- [27] A. Minguzzi and M. P. Tosi, *J. Phys: Condens. Matter (UK)* **9**, 10211-23 (1997).
- [28] S. Stringari, *Phys. Rev. Lett.* **77**, 2360 (1996).

- [29] W. Kohn, Phys. Rev. **123**, 1242 (1961).  
 [30] Jhon F. Dobson, Phys. Rev. Lett. **73**, 2244 (1994).  
 [31] A. Fetter and D. Walecka, *Quantum Theory of Many Particle Systems*, McGraw Hill, New York, 1971.  
 [32] For a similar calculation see, e.g., J. Reidl, G. Bene, R. Graham, and P. Szépfalussy, cond-mat/0010238, (2000).

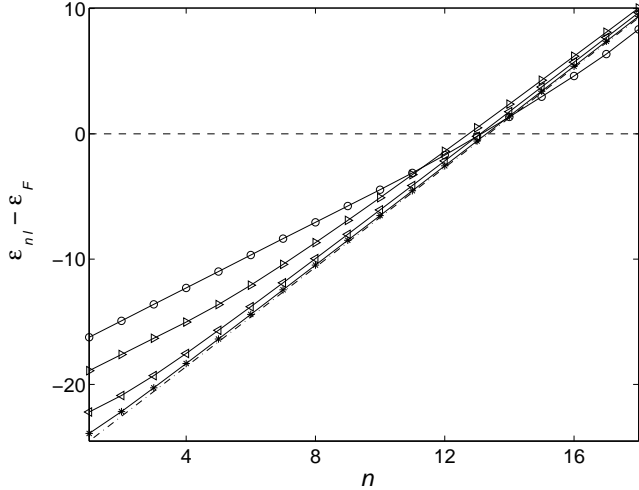


FIG. 1. HF fermionic excitation energies (in units of  $\hbar\omega$ ) for  $N_F = 9880$  and  $l = 0$ . The different symbols indicate different number of bosonic atoms: ( $\circ$ ):  $N_B = 10^6$ ,  $\mu = 32.5\hbar\omega$ ; ( $\triangleright$ ):  $N_B = 10^5$ ,  $\mu = 13.2\hbar\omega$ ; ( $\triangleleft$ ):  $N_B = 10^4$ ,  $\mu = 5.7\hbar\omega$ ; and ( $*$ ):  $N_B = 10^3$ ,  $\mu = 2.9\hbar\omega$ . The dashed-dotted line shows the result for  $g_1 = g_2 = 0$ .

FIG. 2. Monopolar dynamic structure factor in the RPA approximation (in log scale and arbitrary units). Each row corresponds to, from top to bottom,  $N_B = 10^6, 10^5, 10^4, 10^3, 0$ ; while each column, from left to right,  $N_F = 969, 2925, 9880$ . The vertical dotted lines show Stringari's energies [28] for the bosonic system.

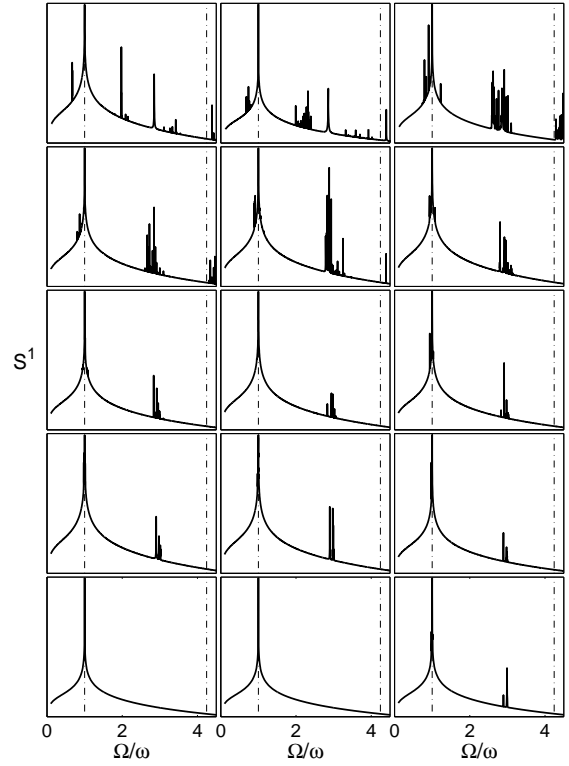
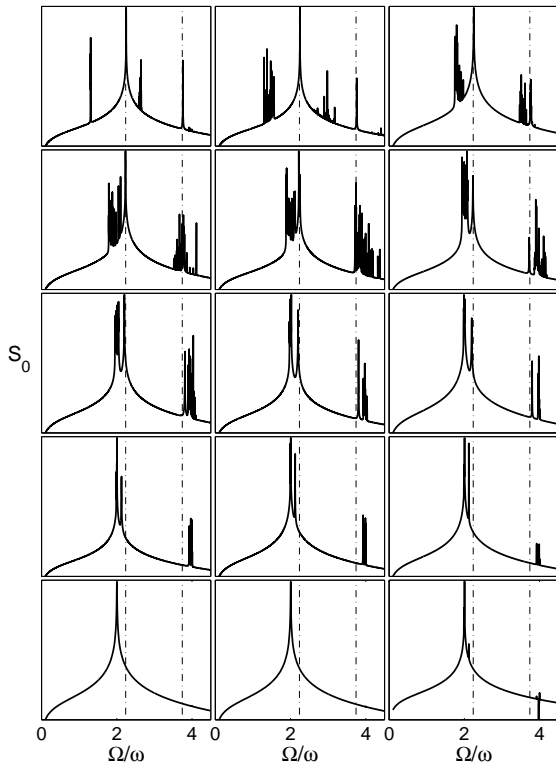


FIG. 3. Idem Fig. 2 for the dipolar response.





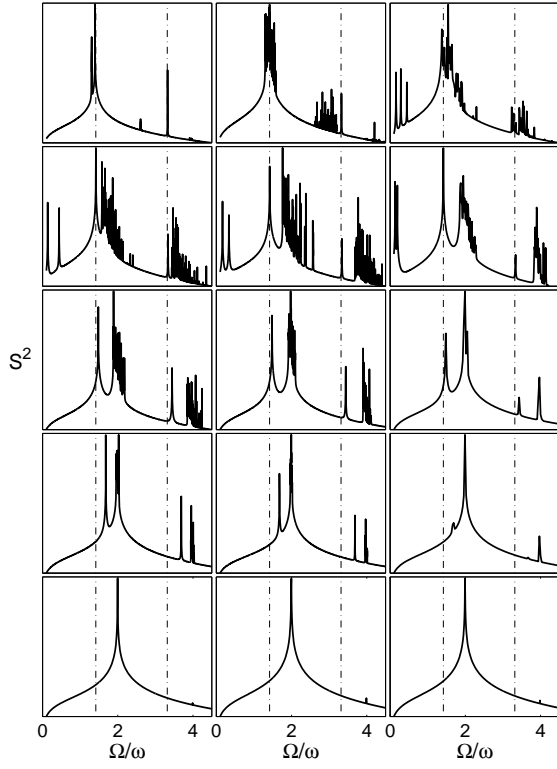


FIG. 4. Idem Fig. 2 for the  $L = 2$  structure factor.

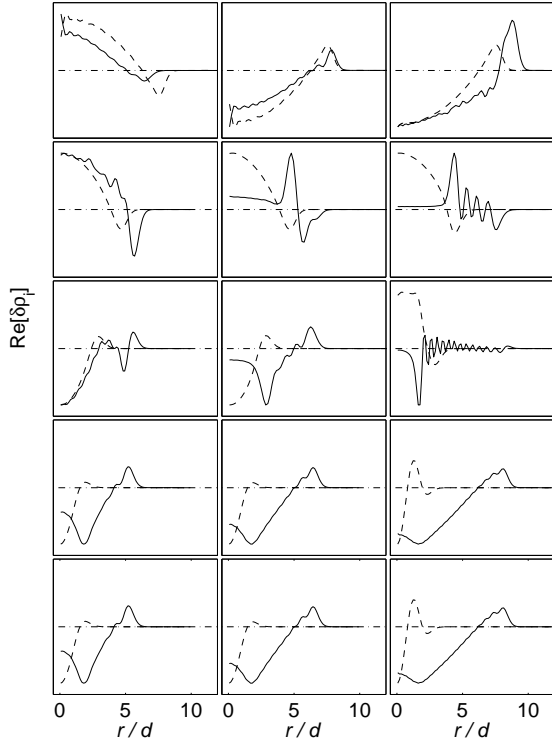


FIG. 5. Transition densities for the  $L = 0$  response (in arbitrary units). The plots show the real parts of the transition densities at the highest peaks in Fig. 2 for each  $(N_F, N_B)$  pair. The solid lines show the fermionic fluctuation while the dashed ones indicate the bosonic part. Each plot corresponds to the same ordering as in Fig. 2. The positions are expressed in terms of the oscillator size  $d = \sqrt{\hbar/m\omega} \approx 1.9\mu\text{m}$ .

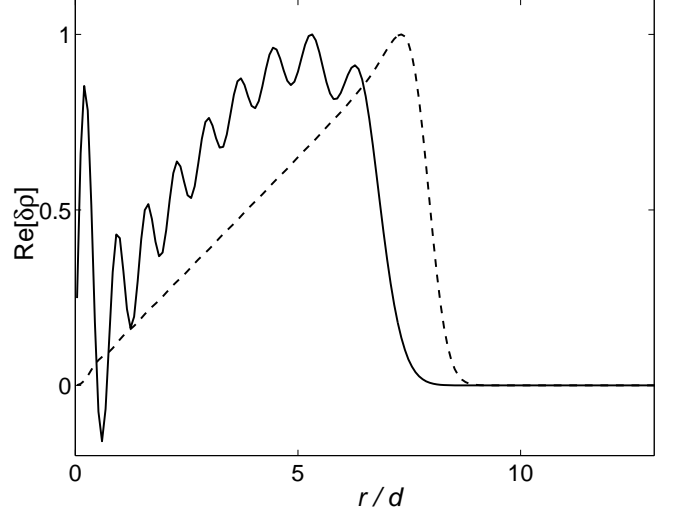


FIG. 6. Dipolar fluctuation at the oscillator frequency for  $N_B = 10^6$  and  $N_F = 969$  (in arbitrary units). Solid and dashed lines correspond to the fermionic and bosonic fluctuations respectively. Each curve has been scaled independently.

TABLE I. Parameters of the stationary densities.  $R_B$ ,  $R_{F\text{eff}}$ ,  $\mu$  and  $\varepsilon_F$  respectively correspond to the radius of the bosonic and fermionic densities and the chemical potential of the bosons and Fermi energy.

$N_B$	$R_B/d$	$R_{F\text{eff}}/d$	$\mu/\hbar\omega$	$\varepsilon_F/\hbar\omega$
$N_F = 969$				
$10^6$	8.3	7.0	32.5	30.5
$10^5$	5.2	6.0	13.0	20.3
$10^4$	3.8	6.0	5.4	18.5
$10^3$	3.0	5.8	2.6	18.5
$N_F = 2925$				
$10^6$	8.4	8.4	32.4	36.1
$10^5$	5.3	7.2	13.1	27.6
$10^4$	4.0	7.0	5.5	26.4
$10^3$	2.5	7.0	2.7	26.4
$N_F = 9880$				
$10^6$	8.0	9.2	32.5	46.0
$10^5$	5.3	8.7	13.2	40.1
$10^4$	3.8	8.5	5.7	39.3
$10^3$	2.4	8.5	2.9	39.3